

PAPER

A comparative study of materials assembled from recombinant K31 and K81 and extracted human hair keratins

To cite this article: Rachael N Parker *et al* 2020 *Biomed. Mater.* **15** 065006

Manuscript version: Accepted Manuscript

Accepted Manuscript is “the version of the article accepted for publication including all changes made as a result of the peer review process, and which may also include the addition to the article by IOP Publishing of a header, an article ID, a cover sheet and/or an ‘Accepted Manuscript’ watermark, but excluding any other editing, typesetting or other changes made by IOP Publishing and/or its licensors”

This Accepted Manuscript is© .



During the embargo period (the 12 month period from the publication of the Version of Record of this article), the Accepted Manuscript is fully protected by copyright and cannot be reused or reposted elsewhere.

As the Version of Record of this article is going to be / has been published on a subscription basis, this Accepted Manuscript will be available for reuse under a CC BY-NC-ND 3.0 licence after the 12 month embargo period.

After the embargo period, everyone is permitted to use copy and redistribute this article for non-commercial purposes only, provided that they adhere to all the terms of the licence <https://creativecommons.org/licenses/by-nc-nd/3.0>

Although reasonable endeavours have been taken to obtain all necessary permissions from third parties to include their copyrighted content within this article, their full citation and copyright line may not be present in this Accepted Manuscript version. Before using any content from this article, please refer to the Version of Record on IOPscience once published for full citation and copyright details, as permissions may be required. All third party content is fully copyright protected, unless specifically stated otherwise in the figure caption in the Version of Record.

View the [article online](#) for updates and enhancements.

A Comparative Study of Materials Assembled from Recombinant K31 and K81 and Extracted Human Hair Keratins

Rachael N. Parker^{1,}, Alexis Trent^{2,*}, Kristina L. Roth¹, Mark E. Van Dyke³, Tijana Z. Grove¹*

1. Department of Chemistry and Macromolecules Innovation Institute, Virginia Tech, Blacksburg, VA 24060
2. Department of Materials Science and Engineering, Virginia Tech, Blacksburg, VA 24060
3. Department of Biomedical Engineering and Mechanics, Virginia Tech, Blacksburg, VA 24060

*Authors contributed equally to this work

Abstract

Natural biopolymers have found success in tissue engineering and regenerative medicine applications. Their intrinsic biocompatibility and biological activity make them well suited for biomaterials development. Specifically, keratin-based biomaterials have demonstrated utility in regenerative medicine applications including bone regeneration, wound healing, and nerve regeneration. However, studies of structure-function relationships in keratin biomaterials have been hindered by the lack of homogeneous preparations of materials extracted and isolated from natural sources such as wool and hair fibers. Here we present a side-by-side comparison of natural and recombinant human hair keratin proteins K31 and K81. When combined, the recombinant proteins (i.e. rhK31 and rhK81) assemble into characteristic intermediate filament-like fibers. Coatings made from natural and recombinant dimers were ~~also~~ compared side-by-side and investigated for coating characteristics and cell adhesion. In comparison to control substrates, the recombinant keratin materials show a higher propensity for inducing involucrin and hence, maturation in terms of potential skin cell differentiation.

KEYWORDS: human hair keratin, biomaterials, recombinant protein, self-assembly, biomimetic coating

Introduction

Biopolymeric scaffolds for tissue engineering and regenerative medicine have garnered much interest over the past few decades[1-11]. Natural biopolymers offer several advantages over traditional implant materials and synthetic polymer-based scaffolds. Natural biopolymeric scaffolds are often constructed from proteins found in the extracellular matrix (ECM) and other native tissues, which contributes to their biocompatibility and minimizes undesirable immune responses. Furthermore, many natural biopolymers have inherent self-assembly properties, functional cell binding motifs, and other important regulatory functions, such as control over cell migration and proliferation that provide them with intrinsic biological activity[6, 10, 12-16]. Conversely, synthetic polymers provide excellent structural support, but lack the intrinsic biological activity[17] and often elicit an unwanted foreign body response[18]. Additionally, synthetic polymers often require chemical modifications in order to improve their biocompatibility and impart biological functions for subsequent use in regenerative medicine applications. Functionalization of scaffolds has proven difficult[19, 20] as it is challenging to control the degree of functionalization and the spatial organization of functional groups[21, 22]. Therefore, natural biopolymers are promising alternatives as biomaterials for regenerative medicine due to their inherent characteristics (e.g. self-assembly, cell binding)[23].

When designing biomaterials for regenerative medicine and tissue engineering, certain criteria should be considered[24]. First, biomaterials need to provide adequate mechanical and structural support. Second, the ability to facilitate and control cellular adhesion, migration, proliferation, and differentiation is essential[25]. Lastly, materials that degrade over time and resorb into the body allow for temporary implants. The ability to control the rate of degradation further enhances the utility of the material as the degradation rate can be tailored to the body's

healing process[26]. Biopolymers such as elastin[16, 27], collagen[12], keratin[28], and silk[29] have all been used for preparation of biomaterials. These biopolymers are characterized by their hierarchical structures and exquisite and tunable mechanical properties[15, 27, 30, 31]. Furthermore, important biological functions, including the ability to promote cellular attachment through specific cell-binding motifs in their primary amino acid sequences, induction of cell proliferation, as well as regulation of cellular differentiation and protein synthesis can be imparted in the process of biomaterial design[27, 32-34].

In the past decade keratin biomaterials have demonstrated utility as a suitable scaffold for tissue engineering and regenerative medicine[35-46]. The inherent self-assembly of keratin biopolymers into fibrous nanostructures allows for processing keratins into materials with excellent mechanical properties. Furthermore, keratins' biological and regulatory functions enhance its biocompatibility and provide useful bioactivity. For example, it has been proposed that keratin biopolymers contain cell binding motifs, specifically the leucine-aspartic acid-valine (LDV) motif[31], and participate in regulation of protein synthesis, cell growth, and proliferation[47, 48]. Consequently, keratin has been employed in bone regeneration[49], wound healing[50], and nerve regeneration[51] applications. A notable example of keratin-based materials demonstrated its utility as a scaffold for bone regeneration through the delivery of recombinant human bone morphogenetic protein 2 (rhBMP-2) via a keratin hydrogel system[49]. Another recent application of keratin-based scaffolds is in drug delivery. Ham et al.[52] used human hair keratins to fabricate hydrogels with controlled degradation profiles to allow for delivery of recombinant human insulin-like growth factor 1. However, despite the apparent utility of keratin biomaterials, structure-property relationship investigations have been mired by the lack of homogeneous biopolymer preparations. During extraction from sources such as hair

and wool fibers, natural keratins are subject to extensive processing conditions that can lead to biopolymer damage. Additionally, the quality of the materials is highly source-dependent. The harsh processing methods required for keratin extraction may result in protein damage leading to alterations in network assembly and undesirable immune response despite the biocompatibility of the biopolymer. Furthermore, major biopolymer components, K31 and K81, co-purify with low molecular weight constituents such as melanin and keratin associated proteins (KAPs).

We have recently reported cloning, expression, and purification of recombinant human hair keratin 31 (K31) and keratin 81 (K81)[53]. K31 and K81 have been identified as the major components of extracted hair keratin materials,[54] which fall into the category of “hard” keratins. Hard keratins are found in epidermal appendages, such as hair, skin, and nails[55]. The defining feature of hair keratins comes from their high cysteine content, which contain 5% or more cysteine residues[56]. This is in stark contrast to epithelial or “soft” keratins, which contain less than 1% of cysteines[56]. Consequently, hard keratins form more rigid structures, compared to the loose bundles formed by soft keratins, which result from extensive intermolecular disulfide bonds formed during assembly. Keratins extracted from natural sources are obtained either through oxidative extraction (so-called keratose or KOS) or through reductive extraction (so-called keratine or KTN). In KOS samples, disulfide bonds are not formed due to the conversion of the cysteine thiol groups to sulfonic acid. KTN cysteines do contain thiol groups and readily form disulfide crosslinks. As a result of this chemical difference, KOS materials are generally less stable than KTN materials as there are no covalent bonds formed in the material[52]. Herein, we present the side-by-side comparison of the solution characterization of recombinant human hair keratins K31 and K81 (rhK31 and rhK81) to KTN. In addition, coatings made from KTN nanomaterials and dimers of recombinant rhK31 and rhK81 were characterized and tested for

their ability to adhere epithelial cells. To that end, we used the epithelial cell line (HaCaT, immortalized keratinocytes) and connective tissue cells (fibroblasts) to follow the focal adhesion formation. Furthermore, we measured involucrin, an early marker of terminal differentiation for keratinocytes.

Materials and Methods

Gene Design and Cloning of Recombinant K31 and K81

Amino acid sequences for K31 and K81 were reverse translated to the resultant DNA sequence and optimized for *E. coli* codon usage. Synthetic genes corresponding to each protein sequence were synthesized by GeneWiz Inc. The gene sequence contained restriction sites for subsequent cloning into the expression vector pProExHtam. BamHI and HindIII, at the 5' and 3' ends, were employed to ligate the gene into the plasmid, following digestion and isolation of the gene from the commercial plasmid puc57. Enzymes were purchased from New England Biolabs (Ipswich, MA). In order to confirm successful cloning of each gene, sequencing was completed by the Virginia Tech Bioinformatics Institute, which confirmed the correct gene sequences were contained in the plasmids. The same procedure was followed for cloning of the K31 and K81 genes. Plasmid pProExHtam contains an N-terminal histidine affinity tag to be used for protein purification.

Protein Expression and Purification of Recombinant Proteins

Recombinant K31 and K81 were expressed using an *E. coli* expression system. The same procedures were followed for both proteins. First, the proteins were expressed in BL21 (DE3) *E. coli* cells. Luria Broth (LB) was used for cell cultures. Cells were grown overnight for 16 hours in 50 ml of media at 37°C with shaking at 250 rpm. LB media was then used to dilute the cells in a 1:100 ratio and cells were grown to an optical density (OD) of 0.6-0.8. Once OD had been

reached, 1 mM isopropyl β -D-1-thiogalactopyranoside (IPTG) was used to induce protein expression, which was completed at 37°C for 4 hours. Cells were then harvested by centrifugation at 5,000 rpm for 15 minutes and subsequently resuspended in lysis buffer pH 8 containing 50 mM Tris HCl, 300 mM sodium chloride, and 1% Tween 20 and then stored at -80°C until purification. An inclusion body purification procedure adapted from Honda et al[57]. was used to extract and purify rhK31 and rhK81. Cell pellets were thawed in a 37°C water bath followed by a 30 minute incubation with 10 mg/ml of lysozyme. Following this step, 10 mM MgCl₂, 1 mM MnCl₂, and 10 μ g/ml of DNase were each added to the protein samples and incubated for an additional 30 minutes. Detergent buffer pH 8 consisting of 20 mM Tris HCl, 200 mM NaCl, 1% Triton X-100, and 2 mM EDTA was then added at an equivalent volume to the sample volume and mixed well before centrifuging for 15 minutes at 5,000 rpm. Following removal of the supernatant, an additional 25 ml of detergent buffer was added to each sample, and the samples were again centrifuged. This procedure was repeated until a tight pellet of inclusion bodies was formed at which time 25 ml of extraction buffer was added. Extraction buffer consists of 10 mM Tris HCl, 2 mM EDTA, 8 M urea, 10 mM β ME, and 1 protease inhibitor cocktail tablet at a pH of 8, and was used to resuspend the inclusion body pellet. The samples were then centrifuged for 1 hour at 16,000 rpm. The resultant supernatant containing the extracted keratin proteins was collected for further purification. rhK31 and rhK81 containing an N-terminal histidine affinity tag were purified using a standard Ni-NTA affinity purification procedure. All buffers used for the purification process also contained 8 M urea to keep proteins in their denatured form until further dialysis.

Keratin Gel Electrophoresis and Western Blot

Sodium dodecyl sulfate-polyacrylamide gel electrophoresis (SDS-PAGE) was used to separate purified protein prior to Western blot analysis. Samples were prepared in a 1:1 ratio of SDS buffer to protein and analyzed on a 10% acrylamide gel. Extracted KTN was diluted at 10mg/ml in sodium phosphate at pH 7.4, and recombinant proteins were prepared at 5 mg/ml. Following SDS-PAGE, proteins were transferred onto nitrocellulose membranes at 0.35A for 2 hours. The membranes were blocked with 5% non-fat dry milk in Tris Buffered Saline with 0.25% Tween 20 (TBST) for 1 hour. Guinea pig anti-human keratin-31 (K31) and guinea pig anti-human keratin-81 (K81) antibodies (Progen Biotechnik, Heidelberg, Baden-Württemberg, Germany) were used as primary probes and were both diluted at 1:2000 in blocking buffer. After 1 hour of incubation, the membranes were washed three times with TBST, submerged into a 1:3000 dilution of the rabbit anti-Guinea pig IgG-HRP (Life Technologies) secondary probe for 1 hour, then again washed three times with TBST. All incubation periods were conducted at room temperature. Pierce ECL Plus substrate (Thermo Fisher Scientific) mix was added to the membranes 3 minutes prior to been imaged in a Fujifilm LAS-3000 Imager (General Electric).

Dialysis

Following affinity purification and molecular weight verification by SDS-PAGE and MS analysis, rhK31 and rhK81 were individually dialyzed out of elution buffer pH 8 containing 300 mM NaCl, 50 mM Tris HCl, 300 mM imidazole, 10 mM β ME, and 8 M urea. In the first step of dialysis the protein was dialyzed against buffer pH 8 with 10 mM Na_2HPO_4 , 75 mM NaCl, 5 mM DTT, and 8 M urea. Four additional dialysis steps were completed with decreasing amounts of urea equal to 6, 4, 2, and 0 M. Each of the steps were completed at 3 hour intervals except for the last step, which was allowed to equilibrate overnight. Keratin proteins that were previously

extracted from human hair fibers and lyophilized were reconstituted and prepared following the same procedure.

Extraction of Natural Keratin Proteins

Natural keratins used for this study were extracted as previously described[58, 59]. Briefly, a sample of human Chinese hair was obtained from a commercial vendor and used as received. 100 grams of hair was placed into a 2 L solution of 0.5 M thioglycolic acid (TGA) adjusted to a pH of 10.5 and shaken at 100 rpm for 15 hours at 37°C. The hair was recovered by sieve and the extraction solution retained. The hair fibers were then placed in a solution of 4 L of 100 mM tris base and shaken at 100 rpm for 2 hours at 37°C. Hair was again recovered by sieve and placed in a freshly prepared 1 L solution of 0.5 M TGA adjusted to a pH of 10.5 and shaken at 100 rpm for 15 hours at 37°C. The resulting extraction solution was retained and the hair was then placed in 2 L of 100 mM tris and shaken at 100 rpm for 2 hours at 37°C. The hair was then recovered by sieve and discarded. The extraction solution was retained and pooled with extraction solutions obtained in previous steps to form a solution of crude keratin extract. The crude extract was clarified of particulate matter by centrifugation through a solids separator running at 30,000 rpm, followed by filtration through a filter membrane with a 20-25 µm average pore size. Keratin nanomaterials were obtained from this clarified crude keratin extract by ultrafiltration using a 100 kDa NLMWCO polysulfone, tangential flow filtration (TFF) cartridge. TFF was conducted with 10 volume washes against a buffer consisting of 10 mM disodium phosphate and 100 mM sodium chloride at pH 9.1, followed by 5 volume washes against purified water. The purified keratin nanomaterial solution was concentrated, titrated to pH 8.5, frozen and freeze dried to produce a keratin nanomaterial powder.

Size exclusion chromatography

A Dionex chromatography system with an Ultimate 3000 UV/Vis detector was used for size exclusion chromatography (SEC). Proteins were detected at 280 nm and analyzed with Chromeleon v6.8 chromatography software. Samples were analyzed following each step of the dialysis process. Each sample was passed through a 0.22 μm filter after a 3 hour equilibration period in the appropriate dialysis buffer. The mobile phase used for each sample corresponds to the relevant dialysis buffer. Samples were analyzed with a flow rate of 0.5 ml/min.

Dynamic light scattering

Dynamic light scattering (DLS) was completed using a Malvern Zetasizer Nano-ZS to analyze the average particle size and size distribution of extracted and recombinant keratin biopolymers in solution. Prior to measurement, samples were filtered using a 0.22 μm filter. Each sample corresponds to steps during the dialysis process, and thus samples contain the corresponding buffer and urea concentration as described in the dialysis section. The Malvern software converts the intensity percent size distribution to volume percent using Mie theory.

Transmission Electron Microscopy

Using a Philips EM420 microscope with an accelerating voltage of 120 kV transmission, electron microscopy (TEM) analysis was performed on extracted and recombinant keratin biopolymers. Samples were prepared using 300 mesh carbon-coated grids purchased from Electron Microscopy Science. Following deposition of the sample on the grid, a 1 minute drying period was allowed before excess sample was removed. All samples were stained using 2% uranyl acetate, with a 30 second drying period. Excess stain was then removed and samples were allowed to air-dry for 24 hours prior to analysis.

Silane Coupling and Protein Deposition

Microscope slides coated with 5nm of titanium (Deposition Research Lab Inc. CO, USA) were cut into 0.8cm by 0.8cm substrates. These substrates were cleaned with 100% ethanol (EtOH) to remove nominal debris. These pieces were then immersed in silane solutions of 5 % 3-Aminopropyltriethoxysilane (a; APTES; TCI America, Portland, OR, USA) in 95:5 EtOH: H₂O solution (v/v) or 10% 3-Isocyanatopropyltriethoxysilane (i; ICPTES; Acros Organics, Geel, Belgium) in 100% EtOH (v/v). The silane solution was filtered with a 0.2µm pore size filter and the substrates placed in gentle agitation for 3 hours, rinsed with 100% EtOH and rinsed with ultrapure water three times. The substrates were subsequently placed into an oven at 110°C for 30 minutes each.

Silane coated substrates were placed in either extracted KTN or dimerized rhK31 and rhK81 recombinant human keratin (rhK) solutions at room temperature (RT) overnight. The KTN solutions were at a 1% concentration and dissolved in 10 mM sodium phosphate at pH 7.4; the rhK was at a concentration of approximately 1 mg/ml in distilled water. Other silane-coated substrates were immersed in human fibronectin (FN; Corning, Corning, NY, USA) at 5µg/ml in phosphate buffered saline (PBS) or bovine collagen I (COL; Corning, Corning, NY, USA), which is only used for elemental analysis and was coated at 5 µg/cm² in 0.01N HCl. Both FN and COL were coated for 1 hour at RT. Gold substrates (not silane-coated) were coated in 1% KTN (w/v) in 10 mM sodium phosphate at pH 7.4 overnight at RT. All substrates were rinsed with ultrapure water, air dried, and exposed to ultraviolet (UV) light for 1 hour. In subsequent sections, the coatings are noted as iKTN for ICPTES-coupled KTN, AuKTN for gold-coupled KTN, iRhK for ICPTES-coupled recombinant dimer, aFN for APTES-coupled fibronectin, aCOL for APTES-coupled collagen, and pTi for plain titanium. From a previous study conducted

in our lab, silane optimization was performed[58], silane coupling selection for FN and COL was adapted from published studies[60-62].

Atomic Force Microscopy (AFM)

Dry substrates were examined in tapping mode on the Veeco BioScope II (Oyster Bay, NY) at RT. Five 2 μ m by 2 μ m spots were analyzed per substrate under a silicon tip (Nanosensors, Switzerland) with curvature of 10 nm and a force constant ranging between 10 - 130 N/m. Surface roughness (RMS) and rendered images were created and analyzed through with the Bruker's Nanoscope software.

Cell Static Adhesion Immunochemistry

Human neonatal primary dermal fibroblast (PCS-201-010; ATCC, Manassas, VA, USA) were grown in RPMI 1640, L-Glutamine, with no sodium pyruvate (Gibco Life Technologies Carlsbad, CA, USA) with an additional 10 % fetal bovine serum (FBS; Gibco Life Technologies Rockville, MD, USA) and 1% penicillin streptomycin (P/S) added. Human keratinocytes HaCaT cells (Catalog #T0020001; AddexBio Technologies, San Diego, CA, USA) were cultured in Dulbecco's Modified Eagle's Medium (DMEM; ThermoFisher, Waltham, MA, USA), with 10% FBS, 1% P/S and 1.5mM sodium pyruvate (ThermoFisher, Waltham, MA, USA). All cells were split 1 to 3 every 2-3 days and incubated at 37°C, 5% CO₂.

For immunochemistry assays, fibroblasts and HaCaT cells were seeded at 10,000 cells/cm² in a 40 μ l serum-free droplet placed onto the substrates and incubated at 37°C for 3 hours, then fixed with 4% paraformaldehyde. Cells were permeabilized, washed, blocked, and focal adhesions were stained with the FAK 100 kit according to the manufacture's protocol (EMD Millipore, Billerica, MA, USA). Dilutions of antibodies were as follows: primary

antibody Anti-Vinculin (1:350), the secondary Alexa Flour 488 (1:300), Phalloidin (1:350) and DAPI (1:1000). Cells were imaged at 10x using a Zeiss LSM 800 confocal microscope.

Involucrin Detection

HaCaT cells were seeded at 10,000 cells/cm² in a 40 µl droplet onto the substrates and incubated at 37°C initially for 3 hours. After 3 hours, a 1 ml solution of media was added and replaced daily for 7 days. For a positive control, HaCaT cells were seeded in high calcium media (2.8mM Ca²⁺). After 7 days of culture, cells were removed using a cell scraper and RIPA buffer. Each whole cell lysate sample and capillary Western blot assay was prepared according to the manufacturer's instructions for the WesTM (ProteinSimple, San Jose, CA, USA). Briefly, cell lysates were prepared with 1 part 5x Fluorescent master mix and 4-part cell lysate, which could be diluted with 0.1x sample buffer, if needed. Involucrin Human Recombinant protein (Thermo Fisher, Waltham, MA, USA) in buffer was used as an analytical control. The ladder is provided but additional sample buffer and dithiothreitol (DTT) is added according to the preparation guidelines. Biotinylated ladder and samples were denatured at 95°C for 5 minutes. Samples, blocking reagent, antibody diluent, primary antibodies, secondary antibodies, streptavidin HRP, wash buffer, and Luminol-peroxide were placed in the provided ProteinSimple well plate. The manufacturer's anti-mouse secondary antibody was used in conjunction with both primary antibodies tested, which included the primary antibody, involucrin (Thermo Fisher, Waltham, MA, USA) (1:1000) and the secondary antibody goat anti-mouse IgG-HRP (1:5000) (Santa Cruz Biotechnology, Dallas, TX, USA). The well plate and one time use capillary insert were placed in the WesTM instrument, where the fully automated process begins. Upon completion, digital images and area peaks were analyzed in ProteinSimple's Compass software.

Smooth Muscle Actin Detection

Fibroblasts were seeded at 10,000 cells/cm² in a 40 µl droplet onto the substrates and incubated at 37°C initially for 3 hours. After 3 hours, a 1 ml solution of media was added and replaced daily for 7 days. For the smooth muscle actin positive control, HeLa cells CCL-2 (ATCC, Manassas, VA, USA) were used on a tissue culture substrate. The same procedure for the Wes system, as described above for involucrin, was followed, except that antibodies used included primary antibody, alpha-SMA (1:500) and secondary antibody, goat anti-mouse IgG-HRP (1:5000) (Santa Cruz Biotechnology, Dallas, TX, USA).

Statistics

Replicates of ≥ 3 were used in all experiments. Graphs were created in either Prism™ (GraphPad Software, San Diego, CA) or Microsoft Excel. Image J and Photoshop (Adobe, San Jose, CA) were used for image processing and analysis. Quantitative data is expressed as mean \pm standard deviation. Differences between experimental groups were assessed by analysis of variance (ANOVA) and a Tukey's post-hoc test for significance using Prism software.

Results and Discussion

Recombinant DNA technology and protein engineering are greatly influencing the next-generation biomaterials landscape. Recombinant protein-based biomaterials provide the structural and mechanical properties of their natural counterparts while offering the potential for creating materials with tunable sequences, and thus tailored and improved characteristics. Cellular binding motifs, degradation sites, and protein fusions exemplify some of the benefits afforded from recombinantly expressed biopolymers[63-67]. Indeed, many protein-based biomaterials, including silk[64, 66, 68, 69], elastin[66, 69-71], collagen[70, 71], and resilin[72] have benefited from recombinant DNA technology. In addition to providing a path to increased

structural and functional complexity of biomaterials, recombinant biopolymers are indispensable in structure-property relationships studies.

Composition and Homogeneity of Recombinant and Extracted Keratin Samples

In addition to K31 and K81, hair fibers contain different types of keratin proteins, including gamma-, alpha-, and beta-keratins.[43] Beta-keratins provide protection to the hair fiber, gamma-keratins serve as a crosslinking agent, and alpha-keratins function as the main structural component[43]. As such, the desired component for fabrication of biomaterials is the alpha-keratin due to its important structural properties. However, through the extraction and purification process it is often difficult to remove the other types of keratin proteins, as well as additional by-products, which results in a heterogeneous mixture following extraction and purification. On the other hand, recombinant proteins are expressed and purified individually. The N-terminal histidine tag enables metal affinity purification allowing for efficient removal of all other proteins and by-products not containing the specific affinity tag. In **Figure 1A** we first visually compare solutions of extracted and recombinant proteins. The purified recombinant protein solution is labeled “1” and the extracted protein solution is labeled “2”. The recombinant protein solution is clear while the extracted solution, even after purification, appears brown. The observed color is from melanin not removed during purification, demonstrating the difficulty of removing compounds that may be tightly complexed to the larger keratin aggregates. In addition, SDS-PAGE analysis of the purified proteins further indicates the improved sample homogeneity of the recombinant keratins. In **Figure 1B**, lanes 1 and 2 represent affinity purified rhK31 (lane 1) and rhK81 (lane 2). A single protein band is present in each, showing that both recombinant proteins have been successfully purified with no observable by-products or unwanted contaminants. However, the extracted KTN sample in lane 3 has many protein components

present, indicating either the difficulty in removing residual hair fiber components or protein degradation, or both.

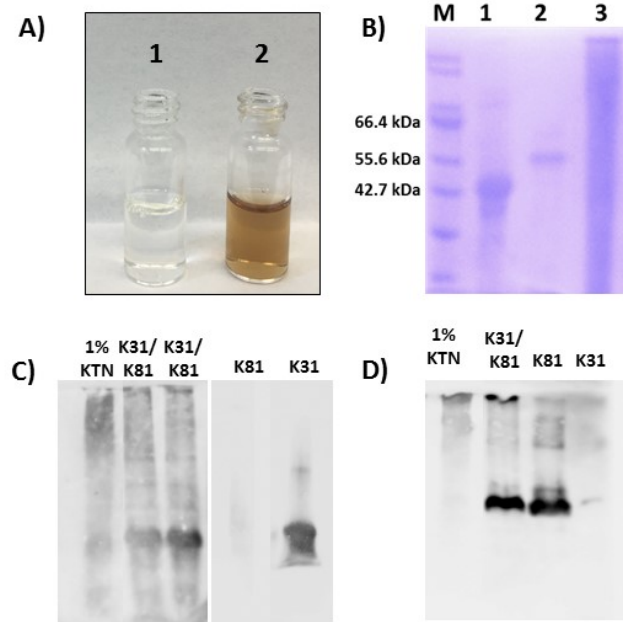


Figure 1. Comparison of purified recombinant and extracted keratins a) picture of purified recombinant (1) and extracted (2) solutions b) SDS-PAGE fractions: M-marker, 1-rhK31, 2-rhK81, 3-Extracted KTN c) Western blot with K31 antibody and d) Western blot with K81 antibody.

To verify the identity of the proteins observed in SDS-PAGE, we conducted a Western blot analysis, which confirmed that the predominant proteins in the recombinant materials preparations were K31 and K81 (**Figures 1C and 1D**, respectively), as expected. Interestingly however, in the extracted sample, the stained bands correspond to higher molecular weights even under denaturing and reducing gel conditions. This suggests the existence of irreversible higher order oligomers in the extracted samples at the same solution conditions in which the recombinant sample is monomeric. The exception is the 1% KTN sample where a band corresponding to the molecular weight of monomeric K31 is observed (**Figure 1C**). Furthermore, not all bands present in SDS-PAGE of the KTN also appear in the Western blot,

signifying the existence of additional proteins in the extracted sample. From the results obtained from SDS-PAGE and Western blot, it appears that recombinant protein production and purification methods provide starting materials of improved homogeneity over that of extracted keratins. However, when rhK31 and rhK81 are combined, bands corresponding to higher molecular weights than monomers appear in Western blots, analogous to extracted KTN sample. Thus, the recombinant heterodimer is capable of heteropolymerization and formation of higher order structures. To further investigate heteropolymerization of rhK31 and rhK81 we utilized SEC and DLS.

Oligomerization States of Recombinant and Extracted Keratins

To prepare samples for SEC analysis, rhK31 and rhK81 were mixed in 8M urea buffer (Materials and Methods). KTN samples were resuspended in buffer of the same composition as the recombinant samples. SEC data obtained in buffer containing 8 M urea shows that both the extracted and recombinant keratin proteins contain structures that are larger than the K31/K81 heterodimer (**Figure 2**). Interestingly, the higher order oligomers are present in both samples even in the presence of a denaturant (urea) and reducing agent (DTT). It is important to note that all samples are passed through a 0.22 μm filter before SEC analysis. Therefore, all structures larger than the filter cut-off will be excluded from this method of analysis.

While five peaks are observed in the recombinant sample chromatogram, the extracted heteropolymer chromatogram contains two broader peaks shifted toward shorter elution times (**Figure 2**). The estimated oligomeric states for each peak (labeled by the red numbers in the **Figure 2**) are shown in **Table 1**.

Table 1. Estimated oligomeric states from SEC analysis.

Peak #	rhK31/K81	KTN
1	Octamer	N/A*
2	Tetramer	Dimer
3	Dimer	----
4	Monomer	----

* Peak elutes in the void volume fraction.

Higher molecular weight peaks 1, 2, and 3 in the recombinant sample overlap with peaks 1 and 3 in the extracted sample suggesting that the K31/K81 octamer, tetramer, and dimer are present in both the extracted and recombinant samples. Peak 1 in the extracted sample, not observed in the recombinant proteins sample, elutes at the time corresponding to the column void volume. Thus, sample components too large to be retained on the column are already present in the extracted sample. At the same time, there is no protein eluting at retention times corresponding to K31 and K81 monomers in the extracted sample. From the SEC analysis we conclude that in the recombinant sample under denaturing conditions the major fraction of the solution is monomeric rhK31 and rhK81 in equilibrium with higher order oligomers. In contrast, the major fraction of the KTN solution corresponds to oligomers larger than octamers and the smallest observable component is a dimer. Dimer observation in the KTN sample is consistent with the formation of the obligate keratin dimer in nature. However, it is interesting that this dimer is resistant to reducing and denaturing conditions.

The presence of larger heteropolymers in the extracted KTN sample, as observed in the SEC, SDS-PAGE, and Western blot analyses, are consistent with the extraction procedure that relies on breaking down preformed, durable keratin-based structures. In order to efficiently extract the desired keratin biopolymers, the extensive network of intermolecular disulfide bonds must be reduced. Thus, the size of sample components acquired from extraction is dependent on

the efficiency with which this network is disrupted, and the resulting higher order structures persist due to covalent interactions that are not affected by the solution conditions. Conversely, recombinant protein production facilitates assembly from each individual component. To further probe the solution behavior of the recombinant and extracted keratins, we used DLS to monitor changes in oligomerization equilibrium as the concentration of denaturant in the sample was decreased.

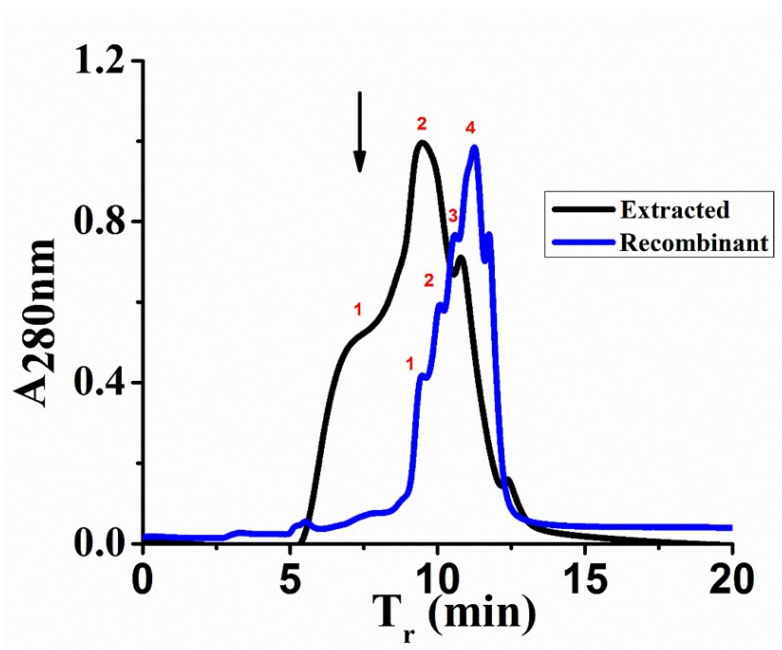


Figure 2. Chromatogram of recombinant (blue) and extracted (black) keratin in 8 M urea obtained from SEC. Red numbers correspond to peak labels listed in table 1.

We performed DLS on aliquots of samples obtained during each dialysis step. As the sample is dialyzed, the concentration of urea in the buffer is reduced in a step-wise manner in order to allow the proteins to return to their native state, and in the case of keratin proteins, to allow for self-assembly to occur. Thus, as the urea concentration decreases, we expect the oligomerization equilibrium to shift towards higher order oligomers and finally fibers. However, all samples are filtered prior to analysis using a 0.22 μm filter. Consequently, any sample components larger than 0.22 μm will not be observed, similar to the SEC. **Figure 3** shows

recombinant (**Figure 3A**) and extracted (**Figure 3B**) heteropolymer samples at 8 M (blue), 4 M (red), and 0 M (black) urea concentrations. Consistent with SEC data, nanostructures present in the KTN sample are larger than in the recombinant sample at the same solution conditions (**Table 2, Figure 3**).

An overlay of the volume percent of recombinant and extracted keratins in 0 M urea is shown in **Figure 3C**. The volume percent distribution provides the relative proportion of the different sample components. The populations detected in the DLS at 0 M urea corresponds to the keratin that has not been incorporated into IF after all denaturant has been removed from the system. The major scattering species in the recombinant keratin sample has an 8 nm hydrodynamic radius, consistent with K31 and/or K81 monomers[73]. The extracted keratin sample is mostly composed of 50 nm oligomers. This is consistent with measurements obtained at each urea concentration, as well as the SEC and Western blot analysis, and further indicates that upon extraction the starting material is not completely reduced to individual proteins.

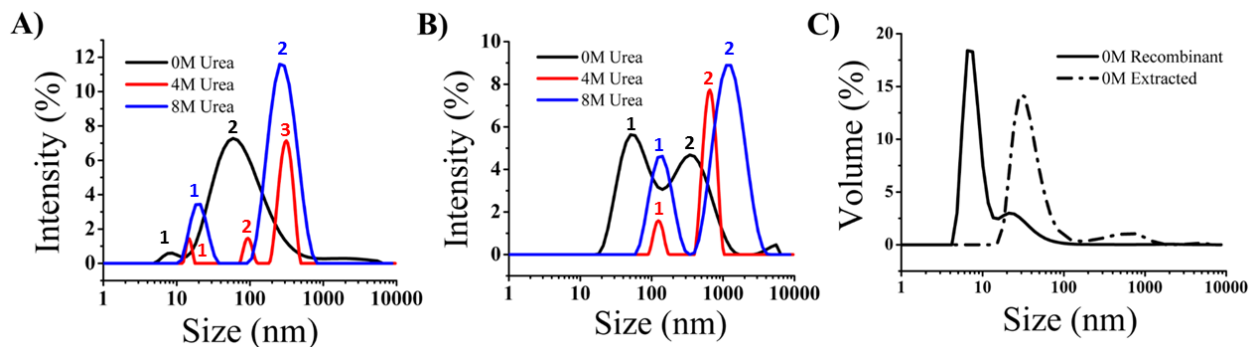


Figure 3. DLS from **A**) recombinant keratin urea series **B**) extracted keratin urea series and **C**) recombinant (solid line) and extracted (dotted line) keratin samples in 0 M urea.

Table 2. Hydrodynamic radius of species present in solution at decreasing urea concentrations.

Urea (M)	Peak #	rhK31/K81 (nm)	KTN (nm)
8	1	18	120
8	2	225	1100
4	1	13	110
4	2	120	900
4	3	460	----
0	1	8	50
0	2	60	295

Nanostructure of Recombinant and Extracted Keratins

One of the essential features of keratin protein materials is their intrinsic capacity for self-assembly. Retaining this important biological feature provides the ability for generation of materials such as films[39], hydrogels[37], and sponges[44]. Self-assembly of keratin IFs is a well-studied process[28, 74]. During IF assembly a dimer composed of one type I (acidic) and one type II (basic) keratin is formed. Following dimer formation, tetramers form through antiparallel alignment of two heterodimers to create a staggered conformation. Subsequent parallel head to tail stacking of tetramers results in protofilaments, which further assemble to form 10 nm diameter IF [28, 75].

In order for recombinant keratin proteins to be viable for use as biomaterials, they too must possess the ability to self-assemble into fibers after expression and purification. Results from solution characterization point to the formation of higher order structures in both the recombinant and extracted samples.

Figures 4A and 4B are representative TEM images of rhK31/K81 nanostructures. The recombinant proteins do self-assemble into standard 10 nm diameter keratin IFs, and further

form large bundles through additional IF interactions. These structures are several microns long and average 150 nm wide. **Figures 4C and 4D** are representative TEM images of the extracted keratin nanostructures. At a 5 mg/ml concentration (same as rhK), the extracted materials readily formed films on the TEM grid. These films appeared featureless and individual fibers or fiber bundles were not observed. Therefore, the extracted samples were diluted to 0.5 mg/ml. This sample concentration resulted in fibers observable by TEM, but the overall number of fibers, in comparison to the recombinant sample, was low. Moreover, these fibers do not have the typical IF morphology. The width of fibers was estimated to be between 70 and 100 nm, with lengths of a few microns (**Figure 4C and 4D**). However, similar to the recombinant sample, some bundling of fibers is apparent (**Figure 4C**).

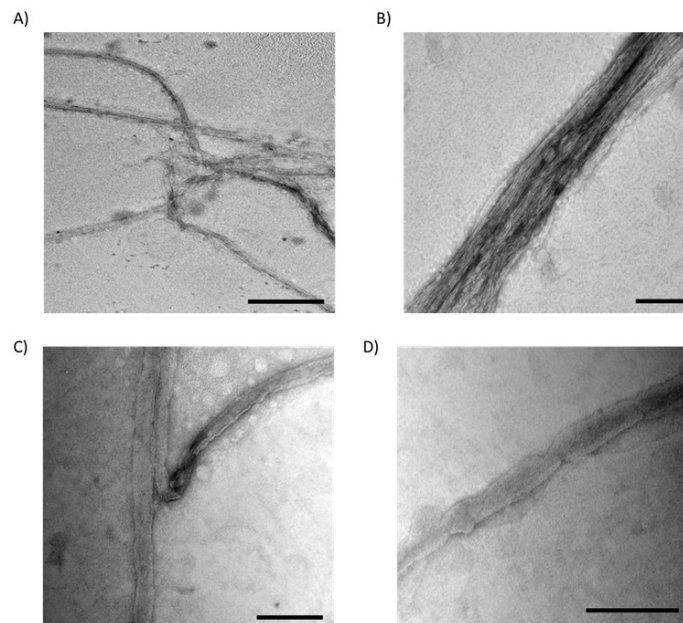


Figure 4. TEM images of recombinant (A-B) and extracted (C-D) keratin proteins. Scale bars are (A) 500 nm and (B-D) 300 nm. All images are stained with 2% uranyl acetate.

Topology of keratin materials

AFM is a commonly used technique with high resolution of approximately 1 Å to characterize topography, which is only limited by thermal and electrical noise[76]. This resolution allows for visualization of molecular structures. AFM confirms that recombinant keratins are able to create a uniform coating, although the roughness is not significantly different than pTi. When observing the topography visually, KTN on gold and recombinant keratins display similarly homogenous surfaces with limited appearance of aggregated features (**Figure 5A**). Here, KTN on gold is used as a positive control as it has been previously been shown that cysteine readily bonds to gold surfaces, a phenomenon that has been used for the formation of self-assembled monolayers or SAMs[77]. KTN attached through a silane coupling layer appears more irregular, suggesting that protein aggregates are present, which is also suggested by the SDS-PAGE, SEC and DLS data. The images are confirmed by roughness measurements that show the KTN on silane is significantly rougher than any of the other test substrates (**Figure 5B**).

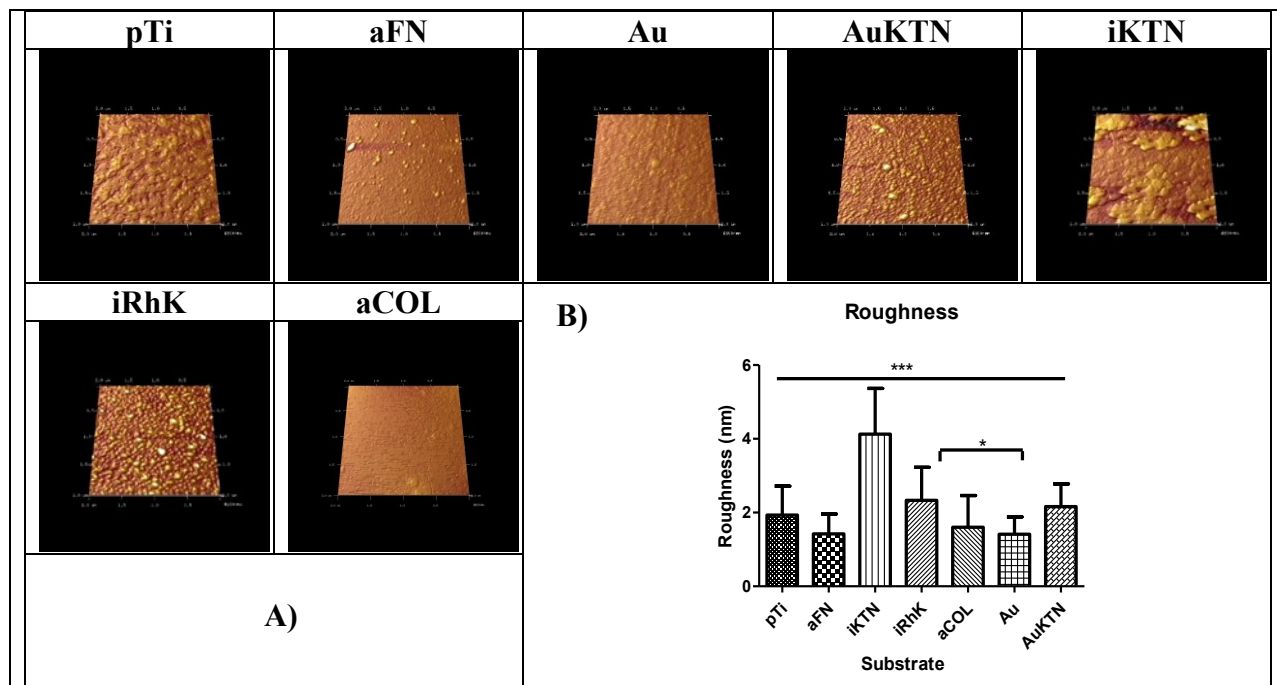
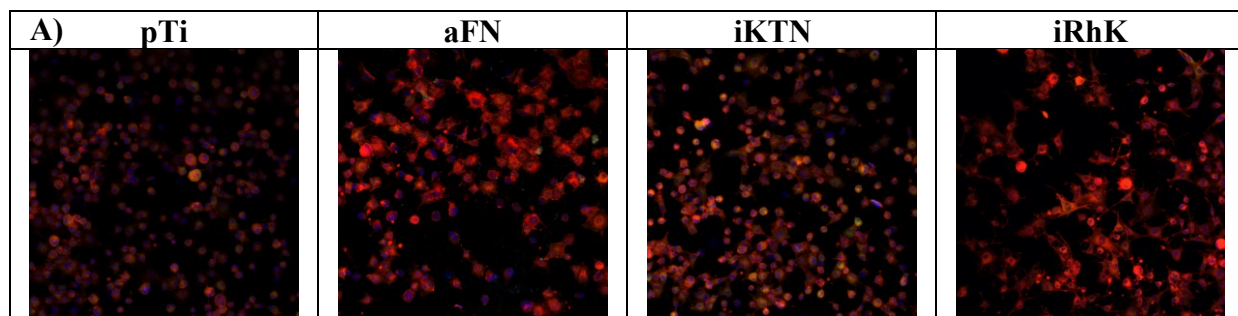


Figure 5. Rendered images of substrates examined by AFM.

Cellular Adhesion Immunochemistry

A cells' biological interactions with coatings can be partially characterized by the growth, maturation and mechanism of attachment. An epithelial cell line (HaCaT) and connective tissue cells (fibroblasts) were used in this study to observe cell attachment. HaCaT cells are immortalized keratinocytes, with their primary *in vivo* cell attachment mediated to the basement membrane[78]. Fibroblasts serve as a connective tissue cell model and attach to the extracellular matrix (ECM), a non-cellular structure that contains fibrous proteins[79]. Focal adhesions create transmembrane communication channels that can activate cell proliferation[80, 81], phenotypic changes[82, 83], and cell signaling cascades[84]. Actin fibers are an indication of focal adhesion formation[81]. **Figures 6 and 7** show the areas of positive actin staining for HaCaT and fibroblast cells, respectively. Although significant differences are not present between the various substrates, the morphologies described through circularity measures exhibit significant changes. In both HaCaT and fibroblast cells, plain Ti, fibronectin, and recombinant keratins allow for the cells to adopt a spread morphology. Cell spreading can indicate that cells perceive the underlying substrate through trans-membrane receptors, even though they may have similar actin protein areas upon staining.



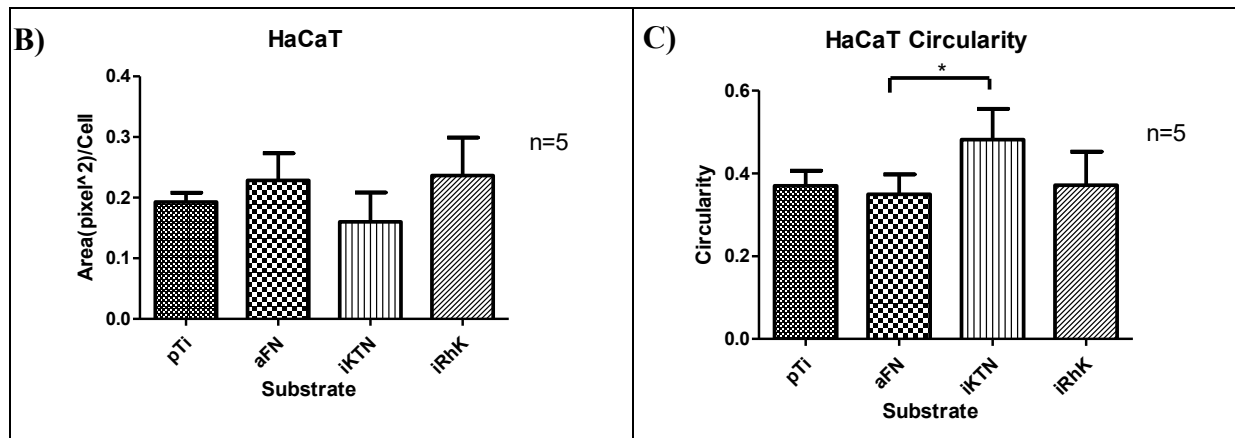


Figure 6. A) HaCaT cells focal adhesions represented by red (Actin), green (vinculin), blue (nucleus). B) Area of Actin staining quantified by ImageJ (n=5). C) Circularity observed by Image J is graphical represented (n=5). Significance is identified by * for $p \leq 0.05$, ** for $p \leq 0.01$, and *** for $p \leq 0.001$. *** ≤ 0.001

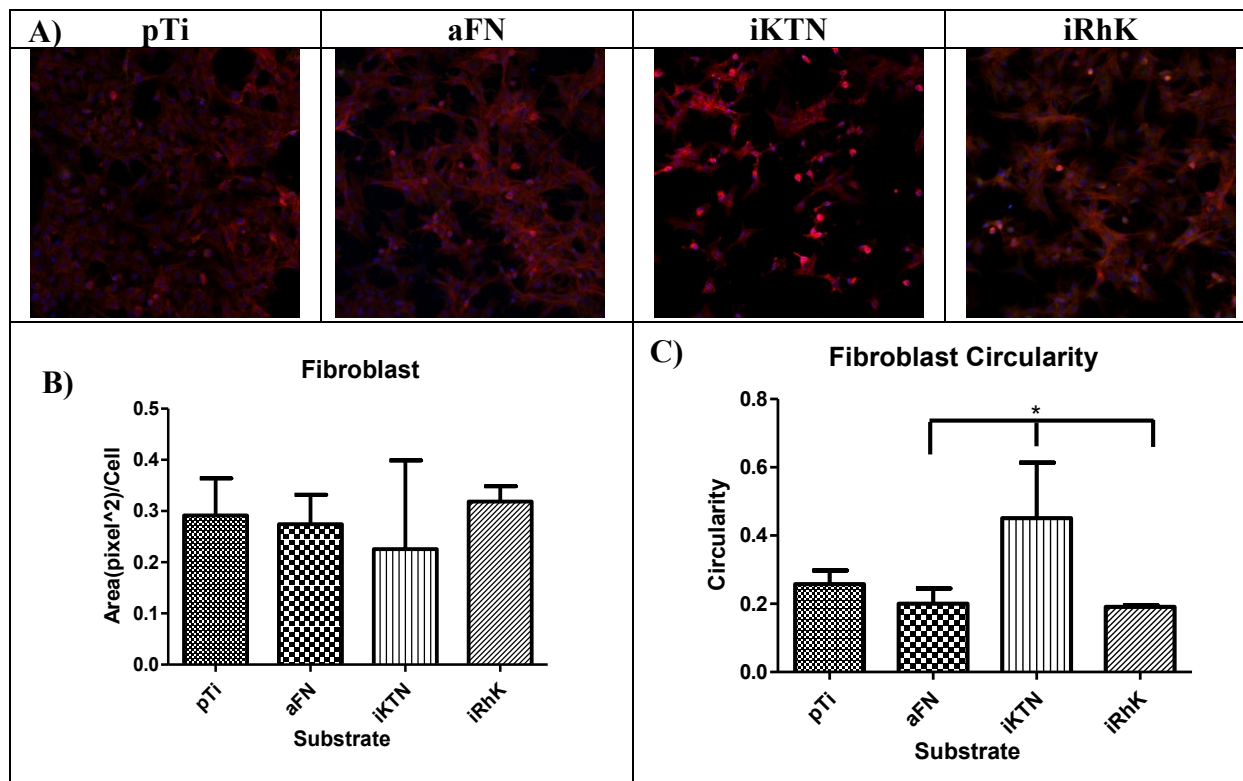


Figure 7. A) Fibroblasts focal adhesions represented by red (Actin), green (vinculin), blue (nucleus). B) Area of Actin staining quantified by ImageJ. C) Circularity observed by Image J is graphical represented. Circularity ranges from zero to one, where one indicates a perfect circle. Significance is identified by * for $p \leq 0.05$, ** for $p \leq 0.01$, and *** for $p \leq 0.001$. *** ≤ 0.001 .

Involucrin and Smooth Muscle Actin Detection

Upregulation of involucrin is an early marker of terminal differentiation for keratinocytes[85], which is defined as the progression of keratinocytes towards a stratified epidermis structure. HaCaT cells exposed to the recombinant keratin coating expressed a higher concentration of the involucrin protein in comparison to other experimental groups (**Figure 8**). During this relatively short-term culture period, the recombinant keratin provokes a response in the HaCaT cells indicating the cells are beginning terminal differentiation. When these cells are transforming from basal cells to granular cells, an upregulation of involucrin occurs, denoting the beginning of keratinization. Other studies have examined involucrin upregulation as a defining test for artificial skin equivalents[86, 87]. These data suggest that the recombinant keratin has a higher propensity for inducing involucrin and hence, maturation in terms of potential skin cell differentiation.

Smooth muscle actin is a definitive characteristic of myofibroblast, which can be induced through mechanotransduction and biochemical cues. Fibroblasts are observed to express SMA on all substrates. Although SMA is a marker for myofibroblasts present in granulation tissue during wound healing[88], substrate stiffness can induce the smooth muscle actin phenotype and cell contractility[89-91]. HeLa cells served as the positive control but were seeded on a tissue culture plate, which does not have an equal stiffness to titanium. This could provide an explanation to why band area and intensity for SMA in HeLa cells is less than all other substrates.

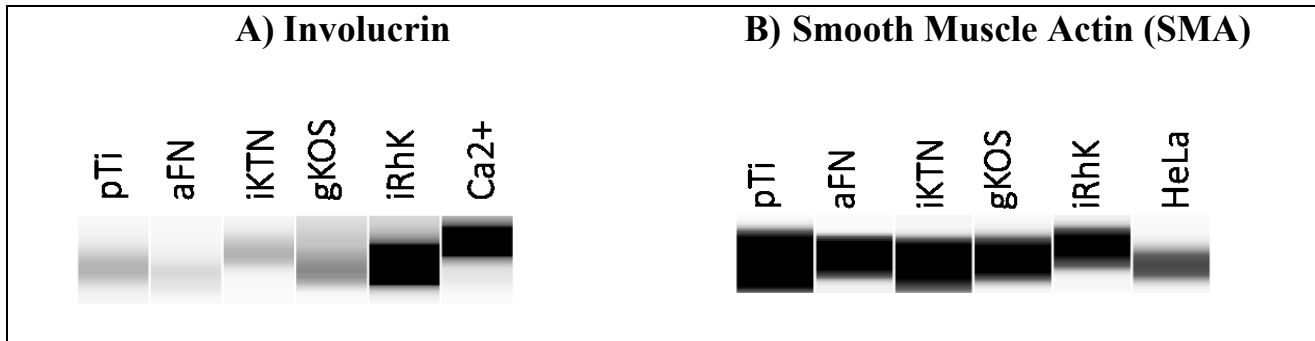


Figure 8. A) **Involucrin.** A digitized Western blot lane view from the ProteinSimple Wes instrument for involucrin including Ca²⁺ induced HaCaT cells, which represent the positive control. B) **Smooth Muscle Actin.** Digitized Western blot for smooth muscle actin in fibroblasts.

Conclusions

Keratin-based biomaterials have been successfully used as scaffolds in regenerative medicine and tissue engineering[42, 52, 92, 93]. However, structure-property studies were impeded by the lack of homogeneity and consistent samples. We have shown here that trichocytic keratins K31 and K81 can be produced recombinantly, resulting in samples of increased homogeneity. Not surprisingly, the composition of extracted versus recombinant materials is shifted towards higher molecular weight oligomers. The distribution of oligomers and their sizes are dependent on the efficiency with which the extensive network of intermolecular disulfide bonds is disrupted in hair fibers, further contributing to the sample heterogeneity.

The recombinant heteropolymer forms standard IF that further associate to create large bundled structures, while extracted keratins fiber did not appear to have the typical IF morphology. Nonetheless, extracted keratins have a remarkable propensity for self-assembly in films that was not observed for recombinant samples under the same conditions. Functional differences in recombinant and extracted keratin composition can also be observed in topography and cellular responses. This further reinforces the notion that recombinant and extracted samples have different compositions. It appears that recombinant keratins, probably due to their relatively

higher level of homogeneity and lack of low molecular weight contaminants, form more uniform coatings, which in turn leads to increased biological activity when compared to KTN.

Design flexibility afforded by recombinant technology will result in multifunctional, dynamic keratin materials. Tailoring of the function, composition, and nanostructure can now be achieved at the amino acid sequence level. Both extracted and recombinant keratin biopolymers provide a promising tool for engineering novel biomaterials with controlled chemical and physical properties, and future work on the fabrication and characterization of these materials will allow for new advances in regenerative medicine, medical device coatings, and tissue engineering.

Abbreviations: rhK31- recombinant human hair keratin 31, rhK81- recombinant human hair keratin 81, IF- intermediate filament, SDS-PAGE- sodium dodecyl sulfate polyacrylamide gel
the Department of Defense Congressionally Directed Medical Research Programs (CDMRP),
grant number W81XWH-15-1-0343; and Virginia Tech-Initiative for Maximizing Student
Development (IMSD), grant number R25GM072767-10

Acknowledgements

The authors would like to thank Virginia Tech, the VT Chemistry Department, the Department of Biomedical Engineering and Mechanics, the Department of Defense Congressionally Directed Medical Research Programs (CDMRP; grant number W81XWH-15-1-0343), and Virginia Tech-Initiative for Maximizing Student Development (IMSD; grant number R25GM072767-10) for funding. We also thank Dr. Sujee Jeyapalina for the gift of the HaCaT cells and for helpful discussions regarding culture and assays for these cells. The authors are also thankful to the Grove and Van Dyke labs for discussions and careful reading of the draft manuscript.

References

- [1] Goldberg M, Langer R, Jia X. Nanostructured materials for applications in drug delivery and tissue engineering. *Journal of Biomaterials Science, Polymer Edition*. 2007;18:241-68.
- [2] Kuratomi Y, Nomizu M, Tanaka K, Ponce ML, Komiyama S, Kleinman HK, et al. Laminin γ 1 chain peptide, C-16 (KAFDITYVRLKF), promotes migration, MMP-9 secretion and pulmonary metastasis of B16-F10 mouse melanoma cells. *British Journal of Cancer*. 2002;86:1169-73.
- [3] Nectow AR, Marra KG, Kaplan DL. Biomaterials for the Development of Peripheral Nerve Guidance Conduits. *Tissue Engineering Part B: Reviews*. 2012;18:40-50.
- [4] Pakulska MM, Ballios BG, Shoichet MS. Injectable hydrogels for central nervous system therapy. *Biomedical Materials*. 2012;7:024101.
- [5] Park S-H, Park SR, Chung SI, Pai KS, Min B-H. Tissue-engineered Cartilage Using Fibrin/Hyaluronan Composite Gel and Its In Vivo Implantation. *Artificial Organs*. 2005;29:838-45.
- [6] Rouse JG, Van Dyke ME. A Review of Keratin-Based Biomaterials for Biomedical Applications. *Materials*. 2010;3:999-1014.
- [7] Schleicher I, Parker A, Leavesley D, Crawford R, Upton Z, Xiao Y. Surface Modification by Complexes of Vitronectin and Growth Factors for Serum-Free Culture of Human Osteoblasts. *Tissue Engineering*. 2005;11:1688-98.
- [8] Silva SS, Mano JF, Reis RL. Potential applications of natural origin polymer-based systems in soft tissue regeneration. *Critical Reviews in Biotechnology*. 2010;30:200-21.
- [9] Stoppel WL, Ghezzi CE, McNamara SL, Iii LDB, Kaplan DL. Clinical Applications of Naturally Derived Biopolymer-Based Scaffolds for Regenerative Medicine. *Annals of Biomedical Engineering*. 2014;43:657-80.
- [10] Vepari C, Kaplan DL. Silk as a biomaterial. *Progress in Polymer Science*. 2007;32:991-1007.
- [11] Wittmer C, Phelps J, Saltzman W, Vantassel P. Fibronectin terminated multilayer films: Protein adsorption and cell attachment studies. *Biomaterials*. 2007;28:851-60.
- [12] Brinckmann J. *Collagens at a Glance*. Topics in Current Chemistry: Springer Berlin Heidelberg; 2005. p. 1-6.
- [13] McKeown-Longo PJ, Panetti TS. Structure and Function of Vitronectin. *Trends in Glycoscience and Glycotechnology*. 1996;8:327-40.
- [14] Pankov R. Fibronectin at a glance. *Journal of Cell Science*. 2002;115:3861-3.
- [15] Parenteau-Bareil R, Gauvin R, Berthod F. Collagen-Based Biomaterials for Tissue Engineering Applications. *Materials*. 2010;3:1863-87.
- [16] Vrhovski B, Weiss AS. Biochemistry of tropoelastin. *European Journal of Biochemistry*. 1998;258:1-18.
- [17] von der Mark K, Park J, Bauer S, Schmuki P. Nanoscale engineering of biomimetic surfaces: cues from the extracellular matrix. *Cell and Tissue Research*. 2009;339:131.
- [18] Anderson JM, Rodriguez A, Chang DT. Foreign body reaction to biomaterials. *Seminars in immunology*: Elsevier; 2008. p. 86-100.
- [19] de Luca AC, Faroni A, Downes S, Terenghi G. Differentiated adipose-derived stem cells act synergistically with RGD-modified surfaces to improve neurite outgrowth in a co-culture model. *Journal of Tissue Engineering and Regenerative Medicine*. 2013;10:647-55.

- [20] Smith Callahan LA, Xie S, Barker IA, Zheng J, Reneker DH, Dove AP, et al. Directed differentiation and neurite extension of mouse embryonic stem cell on aligned poly(lactide) nanofibers functionalized with YIGSR peptide. *Biomaterials*. 2013;34:9089-95.
- [21] Lutolf MP, Hubbell JA. Synthetic biomaterials as instructive extracellular microenvironments for morphogenesis in tissue engineering. *Nature Biotechnology*. 2005;23:47-55.
- [22] Stevens MM. Exploring and Engineering the Cell Surface Interface. *Science*. 2005;310:1135-8.
- [23] Williams DF. On the nature of biomaterials. *Biomaterials*. 2009;30:5897-909.
- [24] Gomes S, Leonor IB, Mano JF, Reis RL, Kaplan DL. Natural and genetically engineered proteins for tissue engineering. *Progress in Polymer Science*. 2012;37:1-17.
- [25] Engler AJ, Sen S, Sweeney HL, Discher DE. Matrix elasticity directs stem cell lineage specification. *Cell*. 2006;126:677-89.
- [26] Kohn J, Welsh WJ, Knight D. A new approach to the rationale discovery of polymeric biomaterials. *Biomaterials*. 2007;28:4171-7.
- [27] Almine JF, Bax DV, Mithieux SM, Nivison-Smith L, Rnjak J, Waterhouse A, et al. Elastin-based materials. *Chemical Society Reviews*. 2010;39:3371.
- [28] Coulombe PA. Elucidating the early stages of keratin filament assembly. *The Journal of Cell Biology*. 1990;111:153-69.
- [29] Altman GH, Diaz F, Jakuba C, Calabro T, Horan RL, Chen J, et al. Silk-based biomaterials. *Biomaterials*. 2003;24:401-16.
- [30] Lu Q, Hu X, Wang X, Kluge JA, Lu S, Cebe P, et al. Water-insoluble silk films with silk I structure. *Acta Biomaterialia*. 2010;6:1380-7.
- [31] Tachibana A, Furuta Y, Takeshima H, Tanabe T, Yamauchi K. Fabrication of wool keratin sponge scaffolds for long-term cell cultivation. *Journal of Biotechnology*. 2002;93:165-70.
- [32] An B, Lin Y-S, Brodsky B. Collagen interactions: Drug design and delivery. *Advanced Drug Delivery Reviews*. 2016;97:69-84.
- [33] Fearing BV, Van Dyke ME. In vitro response of macrophage polarization to a keratin biomaterial. *Acta Biomaterialia*. 2014;10:3136-44.
- [34] Vasconcelos A, Freddi G, Cavaco-Paulo A. Biodegradable Materials Based on Silk Fibroin and Keratin. *Biomacromolecules*. 2008;9:1299-305.
- [35] Belcarz A, Ginalska Gy, Zalewska J, Rzeski W, Ślósarczyk A, Kowalczyk D, et al. Covalent coating of hydroxyapatite by keratin stabilizes gentamicin release. *Journal of Biomedical Materials Research Part B: Applied Biomaterials*. 2009;89B:102-13.
- [36] Dias GJ, Peplow PV, McLaughlin A, Teixeira F, Kelly RJ. Biocompatibility and osseointegration of reconstituted keratin in an ovine model. *Journal of Biomedical Materials Research Part A*. 2009;9999A:NA-NA.
- [37] Hill PS, Apel PJ, Barnwell J, Smith T, Koman LA, Atala A, et al. Repair of Peripheral Nerve Defects in Rabbits Using Keratin Hydrogel Scaffolds. *Tissue Engineering Part A*. 2011;17:1499-505.
- [38] Lee KY, Kong SJ, Park WH, Ha WS, Kwon IC. Effect of surface properties on the antithrombogenicity of silk fibroin/S-carboxymethyl keratine blend films. *Journal of Biomaterials Science, Polymer Edition*. 1998;9:905-14.
- [39] Reichl S. Films based on human hair keratin as substrates for cell culture and tissue engineering. *Biomaterials*. 2009;30:6854-66.

- [40] Reichl S, Borrelli M, Geerling G. Keratin films for ocular surface reconstruction. *Biomaterials*. 2011;32:3375-86.
- [41] Saul JM, Ellenburg MD, de Guzman RC, Dyke MV. Keratin hydrogels support the sustained release of bioactive ciprofloxacin. *Journal of Biomedical Materials Research Part A*. 2011;98A:544-53.
- [42] Shen D, Wang X, Zhang L, Zhao X, Li J, Cheng K, et al. The amelioration of cardiac dysfunction after myocardial infarction by the injection of keratin biomaterials derived from human hair. *Biomaterials*. 2011;32:9290-9.
- [43] Sierpinski P, Garrett J, Ma J, Apel P, Klorig D, Smith T, et al. The use of keratin biomaterials derived from human hair for the promotion of rapid regeneration of peripheral nerves. *Biomaterials*. 2008;29:118-28.
- [44] Tachibana A, Kaneko S, Tanabe T, Yamauchi K. Rapid fabrication of keratin/hydroxyapatite hybrid sponges toward osteoblast cultivation and differentiation. *Biomaterials*. 2005;26:297-302.
- [45] Thilagar S, Jothi NA, Omar ARS, Kamaruddin MY, Ganabadi S. Effect of keratin-gelatin and bFGF-gelatin composite film as a sandwich layer for full-thickness skin mesh graft in experimental dogs. *Journal of Biomedical Materials Research Part B: Applied Biomaterials*. 2009;88B:12-6.
- [46] Yamauchi K, Maniwa M, Mori T. Cultivation of fibroblast cells on keratin-coated substrata. *Journal of Biomaterials Science, Polymer Edition*. 1998;9:259-70.
- [47] Kellner JC, Coulombe PA. Keratins and protein synthesis: the plot thickens: Figure 1. *The Journal of Cell Biology*. 2009;187:157-9.
- [48] Richter JR, de Guzman RC, Van Dyke ME. Mechanisms of hepatocyte attachment to keratin biomaterials. *Biomaterials*. 2011;32:7555-61.
- [49] Kowalczewski CJ, Tombyln S, Wasnick DC, Hughes MR, Ellenburg MD, Callahan MF, et al. Reduction of ectopic bone growth in critically-sized rat mandible defects by delivery of rhBMP-2 from keratine biomaterials. *Biomaterials*. 2014;35:3220-8.
- [50] Burnett LR, Richter JG, Rahmany MB, Soler R, Steen JA, Orlando G, et al. Novel keratin (KeraStat™) and polyurethane (Nanosan®-Sorb) biomaterials are hemostatic in a porcine lethal extremity hemorrhage model. *Journal of Biomaterials Applications*. 2013;28:869-79.
- [51] Apel PJ, Garrett JP, Sierpinski P, Ma J, Atala A, Smith TL, et al. Peripheral Nerve Regeneration Using a Keratin-Based Scaffold: Long-Term Functional and Histological Outcomes in a Mouse Model. *The Journal of Hand Surgery*. 2008;33:1541-7.
- [52] Ham TR, Lee RT, Han S, Haque S, Vodovotz Y, Gu J, et al. Tunable Keratin Hydrogels for Controlled Erosion and Growth Factor Delivery. *Biomacromolecules*. 2015;17:225-36.
- [53] Parker RN, Roth KL, Kim C, McCord JP, Van Dyke ME, Grove TZ. Homo- and heteropolymer self-assembly of recombinant trichocytic keratins. *Biopolymers*. 2017;107.
- [54] de Guzman RC, Merrill MR, Richter JR, Hamzi RI, Greengauz-Roberts OK, Van Dyke ME. Mechanical and biological properties of keratose biomaterials. *Biomaterials*. 2011;32:8205-17.
- [55] Yu J, Yu D-w, Checkla DM, Freedberg IM, Bertolino AP. Human hair keratins. *Journal of Investigative Dermatology*. 1993;101:S56-S9.
- [56] Strnad P, Usachov V, Debes C, Gräter F, Parry DAD, Omary MB. Unique amino acid signatures that are evolutionarily conserved distinguish simple-type, epidermal and hair keratins. *Journal of Cell Science*. 2011;124:4221-32.
- [57] Honda Y, Koike K, Kubo Y, Masuko S, Arakawa Y, Ando S. *In vitro* Assembly Properties of Human Type I and II Hair Keratins. *Cell Structure and Function*. 2014;39:31-43.

- [58] Trent A, Van Dyke ME. Development and characterization of a biomimetic coating for percutaneous devices (in submission). *Material Science and Engineering C*. 2018.
- [59] Van Dyke M, Rahmany M. *Keratin Nanomaterials and Methods of Production*. Google Patents; 2017.
- [60] Chimutengwende-Gordon M, Pendegrass C, Blunn G. Enhancing the soft tissue seal around intraosseous transcuteaneous amputation prostheses using silanized fibronectin titanium alloy. *Biomedical Materials*. 2011;6:025008.
- [61] Middleton C, Pendegrass C, Gordon D, Jacob J, Blunn G. Fibronectin silanized titanium alloy: a bioinductive and durable coating to enhance fibroblast attachment in vitro. *Journal of Biomedical Materials Research Part A*. 2007;83:1032-8.
- [62] Vanderleyden E, Van Hoorebeke L, Schacht E, Dubruel P. Comparative study of collagen and gelatin coatings on titanium surfaces. *Macromolecular Symposia: Wiley Online Library*; 2011. p. 190-8.
- [63] Dinjaski N, Kaplan DL. Recombinant protein blends: silk beyond natural design. *Current Opinion in Biotechnology*. 2016;39:1-7.
- [64] Harris TI, Gaztambide DA, Day BA, Brock CL, Ruben AL, Jones JA, et al. Sticky Situation: An Investigation of Robust Aqueous-Based Recombinant Spider Silk Protein Coatings and Adhesives. *Biomacromolecules*. 2016;17:3761-72.
- [65] Jang Y, Champion JA. Self-Assembled Materials Made from Functional Recombinant Proteins. *Accounts of Chemical Research*. 2016;49:2188-98.
- [66] Rodríguez-Cabello JC, Arias FJ, Rodrigo MA, Girotti A. Elastin-like polypeptides in drug delivery. *Advanced Drug Delivery Reviews*. 2016;97:85-100.
- [67] Zhou M-L, Qian Z-G, Chen L, Kaplan DL, Xia X-X. Rationally Designed Redox-Sensitive Protein Hydrogels with Tunable Mechanical Properties. *Biomacromolecules*. 2016;17:3508-15.
- [68] Spiess K, Lammel A, Scheibel T. Recombinant Spider Silk Proteins for Applications in Biomaterials. *Macromolecular Bioscience*. 2010;10:998-1007.
- [69] Teng W, Cappello J, Wu X. Recombinant Silk-Elastinlike Protein Polymer Displays Elasticity Comparable to Elastin. *Biomacromolecules*. 2009;10:3028-36.
- [70] An B, Abbonante V, Xu H, Gavriilidou D, Yoshizumi A, Bihan D, et al. Recombinant Collagen Engineered to Bind to Discoidin Domain Receptor Functions as a Receptor Inhibitor. *Journal of Biological Chemistry*. 2015;291:4343-55.
- [71] An B, Kaplan DL, Brodsky B. Engineered recombinant bacterial collagen as an alternative collagen-based biomaterial for tissue engineering. *Frontiers in Chemistry*. 2014;2.
- [72] Elvin CM, Carr AG, Huson MG, Maxwell JM, Pearson RD, Vuocolo T, et al. Synthesis and properties of crosslinked recombinant pro-resilin. *Nature*. 2005;437:999-1002.
- [73] Steinert PM, Marekov LN, Fraser RDB, Parry DAD. Keratin Intermediate Filament Structure. *Journal of Molecular Biology*. 1993;230:436-52.
- [74] Steinert PM, Steven AC, Roop DR. Structural Features of Epidermal Keratin Filaments Reassembled in Vitro. *Journal of Investigative Dermatology*. 1983;81:S86-S90.
- [75] Hatzfeld M. The coiled coil of in vitro assembled keratin filaments is a heterodimer of type I and II keratins: use of site-specific mutagenesis and recombinant protein expression. *The Journal of Cell Biology*. 1990;110:1199-210.
- [76] Last JA, Russell P, Nealey PF, Murphy CJ. The applications of atomic force microscopy to vision science. *Investigative ophthalmology & visual science*. 2010;51:6083-94.

- [77] de Guzman RC, Tsuda SM, Ton M-TN, Zhang X, Esker AR, Van Dyke ME. Binding interactions of keratin-based hair fiber extract to gold, keratin, and BMP-2. *PloS one*. 2015;10:e0137233.
- [78] Breitzkreutz D, Schoop VM, Mirancea N, Baur M, Stark H-J, Fusenig NE. Epidermal differentiation and basement membrane formation by HaCaT cells in surface transplants. *European journal of cell biology*. 1998;75:273-86.
- [79] Rhee S, Grinnell F. Fibroblast mechanics in 3D collagen matrices. *Advanced drug delivery reviews*. 2007;59:1299-305.
- [80] Petrie TA, Raynor JE, Reyes CD, Burns KL, Collard DM, García AJ. The effect of integrin-specific bioactive coatings on tissue healing and implant osseointegration. *Biomaterials*. 2008;29:2849-57.
- [81] Yoshigi M, Hoffman LM, Jensen CC, Yost HJ, Beckerle MC. Mechanical force mobilizes zyxin from focal adhesions to actin filaments and regulates cytoskeletal reinforcement. *J Cell Biol*. 2005;171:209-15.
- [82] Fearing BV, Van Dyke ME. Activation of Astrocytes in Vitro by Macrophages Polarized with Keratin Biomaterial Treatment. *Open Journal of Regenerative Medicine*. 2016;5:1.
- [83] Owan I, Burr DB, Turner CH, Qiu J, Tu Y, Onyia JE, et al. Mechanotransduction in bone: osteoblasts are more responsive to fluid forces than mechanical strain. *American Journal of Physiology-Cell Physiology*. 1997;273:C810-C5.
- [84] Maqueda A, Moyano JV, Gutiérrez-López MD, Ovalle S, Rodríguez-Frade JM, Cabañas C, et al. Activation pathways of $\alpha 4\beta 1$ integrin leading to distinct T-cell cytoskeleton reorganization, Rac1 regulation and Pyk2 phosphorylation. *Journal of cellular physiology*. 2006;207:746-56.
- [85] Watt FM. Involucrin and other markers of keratinocyte terminal differentiation. *Journal of Investigative Dermatology*. 1983;81:S100-S3.
- [86] Jung MH, Jung S-M, Shin HS. Co-stimulation of HaCaT keratinization with mechanical stress and air-exposure using a novel 3D culture device. *Scientific reports*. 2016;6:33889.
- [87] Yang EK, Seo YK, Youn HH, Lee DH, Park SN, Park JK. Tissue engineered artificial skin composed of dermis and epidermis. *Artificial organs*. 2000;24:7-17.
- [88] Gabbiani G. The myofibroblast in wound healing and fibrocontractive diseases. *The Journal of pathology*. 2003;200:500-3.
- [89] Hinz B, Celetta G, Tomasek JJ, Gabbiani G, Chaponnier C. Alpha-smooth muscle actin expression upregulates fibroblast contractile activity. *Molecular biology of the cell*. 2001;12:2730-41.
- [90] Jones C, Ehrlich HP. Fibroblast expression of α -smooth muscle actin, $\alpha 2\beta 1$ integrin and $\alpha v\beta 3$ integrin: influence of surface rigidity. *Experimental and molecular pathology*. 2011;91:394-9.
- [91] Solon J, Levental I, Sengupta K, Georges PC, Janmey PA. Fibroblast adaptation and stiffness matching to soft elastic substrates. *Biophysical journal*. 2007;93:4453-61.
- [92] Pace LA, Plate JF, Mannava S, Barnwell JC, Koman LA, Li Z, et al. A Human Hair Keratin Hydrogel Scaffold Enhances Median Nerve Regeneration in Nonhuman Primates: An Electrophysiological and Histological Study. *Tissue Engineering Part A*. 2013;131115063659000.
- [93] Tomblyn S, Pettit Kneller EL, Walker SJ, Ellenburg MD, Kowalczewski CJ, Van Dyke M, et al. Keratin hydrogel carrier system for simultaneous delivery of exogenous growth factors and muscle progenitor cells. *Journal of Biomedical Materials Research Part B: Applied Biomaterials*. 2015;104:864-79.